

# Cosmic crystallography

R. Lehoucq<sup>1</sup>, M. Lachièze-Rey<sup>1,2</sup> and J.P. Luminet<sup>3</sup>

<sup>1</sup> CE-Saclay, DSM/DAPNIA/Service d'Astrophysique, F-91191 Gif sur Yvette cedex, France

<sup>2</sup> CE-Saclay, DSM/DAPNIA/Service d'Astrophysique, CNRS-URA 2052, F-91191 Gif sur Yvette cedex, France

<sup>3</sup> Département d'Astrophysique Relativiste et de Cosmologie, CNRS-UPR 176, Observatoire de Paris-Meudon, France

september 1995

**Abstract.** We assume that the Universe has a non trivial topology whose compact spatial sections have a volume significantly smaller than the horizon volume. By a topological lens effect, such a “folded” space configuration generates multiple images of cosmic sources, e.g. clusters of galaxies. We present a simple and powerful method to unveil non ambiguous observational effects, independently of the sign of the curvature and of the topological type. By analogy with techniques used in crystallography, we look for spikes in the pair separation histogram between cosmic objects in 3-D space. The spikes due to multi-connectedness should stand out dramatically. Moreover, their positions and their relative amplitudes would be definite signatures of the topological type and of the underlying geometry. Such a statistical method would thus reveal the shape of space. As illustrative examples, we perform numerical simulations in  $\Omega = 1$  Friedmann universes with the six possible closed orientable topologies, which prove the efficiency of our method. Presently available 3D catalogs of galaxy clusters are not deep enough to test our method at sizes greater than lower limits  $\approx 600 h^{-1}$  Mpc previously obtained by other methods. With extensive redshift surveys currently in progress the situation may change in the next decade.

**Key words:** cosmology: large scale structure of Universe, topology

## 1. Introduction

It is presently believed that our Universe is correctly described by one of the spatially homogeneous and isotropic Friedmann-Lemaître models. Their spatial sections are of the elliptical, Euclidean or hyperbolic type according to the sign of their constant spatial curvature. Most studies in the field assume that the topology of space is simply-connected, but the possibility of a non trivial topology becomes an increasingly popular topic in theoretical and observational cosmology (for a review, see Lachièze-Rey and Luminet 1995, hereafter LaLu95 and references therein; also Fagundes 1995).

For the simply-connected models, the finite or non finite character of space is linked to the sign of spatial curvature: elliptical models have finite volumes whereas Euclidean and hyperbolic models have infinite volumes. In that case the question of the extension of space (one of the oldest cosmological problems, going back to almost twenty five centuries) is reduced to the estimation of the average mass-energy density of the Universe (including a possible cosmological constant's contribution). The situation is different for multi-connected models (Ellis 1971), since the three geometries of constant curvature admit compact space forms (although the elliptical family do not admit non compact ones).

Present observations do not clearly indicate the value of the spatial curvature of the Universe, neither whether space is simply or multi-connected. However observational effects are expected if the physical space is compact in at least one direction and if its corresponding size is smaller than the horizon distance. We call such a space “small folded”. Two of us (LaLu95) published a critical review of the various methods already proposed to check the cosmic topology; most of them present at least one of the following drawbacks: (i) they apply to one particular type of multi-connectedness only, for instance the torus like topology; (ii) they rest on strong assumptions about the cosmological

---

*Send offprint requests to:* J.P. Luminet

model, for instance an Einstein–de Sitter universe, or on the properties of a peculiar population of cosmic objects, for instance quasars; (iii) they do not provide an unambiguous signature of multiconnectedness.

In this article we propose to test if space is a small folded one by studying the histogram of pair separations between cosmic sources. Our method is an improved version of the construction of the correlation function of clusters already pioneered by Schvartsman and his group (references in LeLa95). It is free from the preceding drawbacks and is independent of preliminary assumptions about the topological type.

We recall general properties of multi-connected universe models in section 2. We present the pair separation histogram method in section 3. We check its validity on simulated universe models in section 4. We perform the test on a 3D catalog of galaxy clusters and draw conclusions in section 5.

## 2. Small folded universes

### 2.1. General properties

Mathematically, a space is simply-connected if every loop can be continuously shrunk to a point. If not, the space is multi-connected. A multi-connected space is conveniently described by its fundamental polyhedron  $F$  and its holonomy group  $\Gamma$ .  $F$  is convex, with a finite number of faces which are identified by pairs.  $\Gamma$  is generated by transformations which carry a face to its homologous one. The latter are isometries without fixed point. The fundamental polyhedron is transformed into its images  $\gamma F$  by the holonomies  $\gamma \in \Gamma$ . The reunion of the  $\gamma F$ 's form a regular tiling of the so-called universal covering space. A simply-connected space is identical to its universal covering space, whereas a multi-connected space is the quotient of the universal covering space by the holonomy group of its fundamental polyhedron.

Applied to the spatial sections of cosmological models, the fundamental polyhedron indeed identifies with the physical space, in which objects like galaxies or clusters are located, whereas the universal covering space identifies to  $\mathbb{S}^3$ ,  $\mathbb{R}^3$  or  $\mathbb{H}^3$  according to the sign of the curvature (we assume, as usual in cosmology, homogeneity and local isotropy of space).

A given cosmic object lies at a given position in physical space, i.e. in  $F$ . Its images under  $\Gamma$  lie in the universal covering space. The latter is thus the “observer’s world”, which may drastically differ from the real world. As an example, the observer may see several images of the same cosmic object if  $F$  is smaller than the particle horizon distance in at least one space direction. This gives rise to the appellation of “small folded” universe. By convention we call the nearest source the “original” and the other images “ghosts”.

Small folded universe models are easier to understand with the following remarks: (i) although it is not the physical space, the universal covering space in a given multi-connected Friedmann–Lemaître model has exactly the same properties than the physical space of the corresponding simply-connected model; (ii) a ghost object in the universal covering space of a multi-connected model has the same properties (observed distance, redshift, age) as the object located at the same position in the real space of the corresponding simply-connected model.

A multi-connected universe model is characterized by some spatial scales associated to the fundamental polyhedron. Let us call  $\alpha$  its smallest length. In a non flat space, characterized by its present curvature radius  $R_0$ , the ratio  $\alpha/R_0$  is geometrically constrained to specified values (LaLu95). For instance it has a maximum (resp. minimum) value if  $k > 0$  (resp.  $k < 0$ ), whereas it remains arbitrary in flat space. The fundamental polyhedron also involves another scale  $\beta$ , the maximum length inscriptible in it (this is for instance the diagonal for a parallelepipedic fundamental polyhedron, which characterizes the hypertorus). This is also the maximum distance between 2 images of the same object belonging to adjacent cells.

Directly observable effects are expected if  $\alpha$  or  $\beta$  are smaller than the horizon size. By construction, only original images (no ghosts) are present up to a distance  $\alpha/2$ . Between  $\alpha/2$  and  $\beta/2$  there is a mixture of original and ghost images. Beyond  $\beta/2$  there are only ghosts. Of course, the smaller the basic cell, the easier to detect topological effects. The number of potential ghosts depends on the cosmic parameters and on the topology. For a given object, there are as much potential ghosts as cells in the universal covering space; their number is thus finite in the case of positive constant spatial curvature, infinite otherwise. An obvious limitation is that only ghosts nearer than the particle horizon may be seen, so that their number is at most equal to the number of cells within the particle’s horizon. In addition, the number may be drastically reduced by the fact that in practice, we can only observe below some magnitude or redshift cut-off, depending on the type of objects (galaxies, clusters, etc.), on the instrumentation and various other limitations.

## 2.2. Observational constraints

No direct observation presently indicates that our universe is a small folded one. By direct observation we mean recognition of ghost images of known cosmic objects or configurations. This places lower limits on the size of the physical space according to the type of objects. Some tests involve the diffuse cosmic microwave background, other the discrete sources such as quasars or clusters. From the COBE/DMR results, Stevens et al. (1993), Starobinsky (1993) and de Oliveira-Costa & Smoot (1995) have claimed to rule out multi-connectedness on sub-horizon scales. However their results rely onto various disputable assumptions, for instance the absence of strong reionization after recombination (see section 12.3 in LaLu95 for an extended discussion). Fagundes (1995) tried to fit the cold and hot spots in COBE/DMR maps of the cosmic microwave background with the predictions of some compact hyperbolic models with  $\Omega < 1$ , whereas Jing and Fang (1994) fitted the two-point angular correlation function of the cosmic microwave background. At present time, limits derived from the cosmic microwave background observations are not model independent and cannot be considered as definitive yet. Thus it remains valuable to check the cosmic topology with a different method.

Tests which involve discrete sources must consider populations of objects extending deep enough in space to check large dimensions. Quasars seem potentially interesting, but their estimated lifetime is short compared to the expected time necessary for a light ray to turn around a small folded universe: a typical lifetime less than  $\approx 10^8$  yrs would only allow to investigate scales smaller than 200 Mpc.

The observations of clusters and superclusters of galaxies seem more adapted. They have led to the limits  $\alpha > 60 h^{-1}$  Mpc (Gott 1980) and  $\beta > 600 h^{-1}$  Mpc (Sokoloff and Schvartsman 1974, Fang & Liu 1988), where  $h$  is the Hubble constant in units of  $100 \text{ km sec}^{-1} \text{ Mpc}^{-1}$ . To our knowledge, they are the best observational constraints derived from discrete sources. They leave room for many observable effects in a folded universe. To get a qualitative idea, let us assume an Einstein-de Sitter model (zero curvature) with a cubic hypertorus of length  $L$  as fundamental cell. The redshift-distance relation is  $d(z) = d_H (1 - (1 + z)^{-1/2})$ , where  $d(z)$  is the distance in the universal covering space, and  $d_H = 2c/H_0 \approx 6000 h^{-1}$  Mpc is the horizon distance. Table 1 gives the multiplication factor, namely the number of ghost images of a given original object, for various cell sizes compatible with present observations.

**Table 1.** Multiplication of images in a cubic hypertorus universe with fundamental lengths  $L$ , in units of  $h^{-1}$  Mpc.  $z_\alpha$  is the redshift until which there are only originals,  $z_\beta$  the redshift beyond which there are only ghosts,  $M(d_H)$  the multiplication factor until the horizon distance  $d_H$ ,  $M(z)$  the multiplication factors until various redshift cut-offs. Magnitude limitations, absorption, luminosity evolution and other observational biases are neglected.

$L$	$z_\alpha$	$z_\beta$	$M(d_H)$	$M(4)$	$M(1)$	$M(0.5)$
500	0.09	0.16	7000	1200	180	45
1000	0.19	0.37	900	150	23	5
1500	0.31	0.63	279	45	7	1.5
2000	0.44	0.98	110	20	3	–
2500	0.60	1.45	60	10	1.5	–

The limits mentionned above are mainly derived from the absence of ghosts of peculiar objects (the Milky Way, some known clusters or superclusters). However some ghosts would be unobservable for various reasons not linked to the geometry (absorption by dust, difficulty to recognize the object, etc.). This motivates a search for statistical tests which would be less dependent on peculiar objects and would exploit the largest amount of the information contained in 3-D catalogs.

Different methods have been proposed, such as the search for a periodic or quantized distribution of objects in redshift or in distance (Fang 1990). For instance, it may be tempting to invoke multi-connectedness for explaining the apparent periodicity observed by Broadhurst et al. (1990) in a pencil-beam catalog of galaxies. But Park and Gott (1991), among others, were able to reproduce comparable results in ordinary simply-connected universe models. As emphasized in LaLu95, such tests cannot be decisive, and our numerical simulations below confirm this point of view.

## 3. A pair separations histogram for testing cosmic topology

Since the above methods do not provide a clear signature of multi-connectedness, we propose a more general one, independent on the peculiar topology or on the peculiar cosmic objects. In this purpose, we go back to the basic

property of folded universes: each image of a given object is linked to each other one by the holonomies of space. Without knowing the geometry or the topology we do not know what are these holonomies, but we know that they are isometries. Therefore, any pair of images comprising an original and one of its ghosts, or two ghosts of the same object, reflects an isometry of space. We call such a pair a gg-pair. A signature of multi-connectedness would be that, among all pairs of images, a significant proportion are gg-pairs. So the question is: how to extract gg-pairs from ordinary pairs? The answer is provided by the histogram of space separations between all pairs of images in a 3-D catalog, as we see now in more detail.

A topology is characterized by its holonomies, which are combinations of the generators  $\{\gamma_k\}$  of the holonomy group. Each generator  $\gamma_k$  is itself an holonomy, to which is associated an identification length  $\lambda_k$  related to the size of the fundamental polyhedron. For instance, in toroidal models the  $\lambda_k$  are equal to the edges  $L_e$ ,  $L_a$  and  $L_u$  of the parallelepipedic fundamental polyhedron. More generally, the  $\lambda_k^2$  are related to  $L_e^2$ ,  $L_a^2$  and  $L_u^2$  by linear relations involving integer coefficients.

All the gg-pairs corresponding to the same generating holonomy  $\gamma_k$  are characterized by the same separation  $\lambda_k$  (in proper comoving distance units). Thus, if we draw the histogram of the pair separations, or rather the squared separations, these gg-pairs will emerge from ordinary pairs as a spike located at the position  $\lambda_k^2$ . In addition to the generating holonomies, other holonomies appear as compositions of them, also giving characteristic spikes. They also generate gg-pairs with squared separations

$$\Lambda_i^2 = \sum N_k \lambda_k^2, \quad (1)$$

where the  $N_k$  are integers.

The principle of our test is to recognize the presence of spikes associated to these values, in a catalog of observed cosmic sources. Let us assume that our catalog of  $N$  objects (thus containing  $N(N-1)/2$  pairs) has a characteristic volume about  $F$  times that of the fundamental polyhedron. The latter thus contains about  $N/F$  (original) objects, the other being ghosts. Each ghost  $g_1$  (excepted near the edges) is transformed by the holonomy generator  $\gamma_k$  to give an other ghost  $g_2$ , their separation being  $\lambda_k$ . Thus, we expect about  $N$  (in fact less because of edge effects) corresponding gg-pairs with separation  $\lambda_k$ , which will emerge as a spike above the background contribution of ordinary pairs. If 2 or 3 identification lengths are equal, this number is to be multiplied by 2 or 3 and the corresponding spike will be enhanced.

In a small folded universe, the spikes would be observable and provide a signature of multi-connectedness, like in a crystallographic lattice. The integer values  $N_k$  would be measurable and (together with the relative heights of the spikes) indicate exactly the type of topology involved. This is illustrated in the next section. Note that the practical calculus of separations depending on the curvature of space, the analysis has in principle to be performed in the three different cases  $k = -1, 0, 1$ . However, the Euclidean approximation applies well when the catalog does not extend too deeply.

## 4. Simulated folded universes

### 4.1. Locally Euclidean models

In order to check the validity of our test, we have generated simulated catalogs of a distribution of objects (typically, galaxy clusters or quasars) in a multi-connected universe. For simplicity, we chose a flat Friedmann-Lemaître (Einstein-de Sitter) universe, whose universal covering space is  $\mathbb{R}^3$ . We investigated the six compact oriented topologies, denoted  $\mathcal{T}_1$  to  $\mathcal{T}_6$  (see Wolf 1984, and Fig. 17 of LaLu95 for a pictorial representation). Each type is specified by a fundamental polyhedron with three edge lengths  $L_e$ ,  $L_a$ ,  $L_u$ , and the structure of its holonomy group. The latter may be characterized by the formulae identifying the coordinates  $\mathbf{r} = (x, y, z)$  and  $\mathbf{r}' = (x', y', z')$  of a gg-pair :

for types  $\mathcal{T}_1, \mathcal{T}_2, \mathcal{T}_3$

$$\mathbf{r}' = R_{Oz}(\alpha_i) \mathbf{r} + \begin{pmatrix} n_e L_e \\ n_a L_a \\ n_u L_u \end{pmatrix} \quad (2)$$

for types  $\mathcal{T}_4$

$$\mathbf{r}' = R_{Ox}(n_e\pi)R_{Oy}(n_a\pi)R_{Oz}(n_u\pi) \mathbf{r} + \begin{pmatrix} n_e L_e \\ n_a L_a \\ n_u L_u \end{pmatrix} \quad (3)$$

for types  $\mathcal{T}_5, \mathcal{T}_6$

$$\mathbf{r}' = R_{Oz}(\alpha_i) \mathbf{r} + \begin{pmatrix} 1 & -1/2 & 0 \\ 0 & \sqrt{3}/2 & 0 \\ 0 & 0 & 1 \end{pmatrix} \begin{pmatrix} n_e L_e \\ n_a L_a \\ n_u L_u \end{pmatrix} \quad (4)$$

where  $R_{Ox}(\theta)$ ,  $R_{Oy}(\theta)$  and  $R_{Oz}(\theta)$  are the rotation matrices of angle  $\theta$  about the three coordinates axis,  $n_e, n_a$  and  $n_u$  are integers denoting the position of a cell in the universal covering space,  $L_e, L_a, L_u$  and  $\alpha_i$  are given in Table 2.

**Table 2.** The six locally Euclidean, closed, oriented 3-spaces

Type $\mathcal{T}_i$	Fundamental polyhedron	$\alpha_i$
$\mathcal{T}_1$	parallelepiped, $L_e, L_a, L_u$	0
$\mathcal{T}_2$	parallelepiped, $L_e, L_a, L_u$	$\pi n_u$
$\mathcal{T}_3$	parallelepiped, $L_e = L_a, L_u$	$\pi/2 n_u$
$\mathcal{T}_4$	parallelepiped, $L_e, L_a, L_u$	–
$\mathcal{T}_5$	hexagonal prism, $L_e = L_a, L_u$	$2\pi/3 n_u [\text{mod } 3]$
$\mathcal{T}_6$	hexagonal prism, $L_e = L_a, L_u$	$2\pi/6 n_u [\text{mod } 6]$

Type  $\mathcal{T}_1$  corresponds to the well known hypertorus. Types  $\mathcal{T}_3, \mathcal{T}_5$  and  $\mathcal{T}_6$  constrain two lengths to be equal. The volume of a cell (also of the physical space) is  $V = L_e L_a L_u$  for types  $\mathcal{T}_1$ – $\mathcal{T}_4$ , and  $V = 3\sqrt{3}/2 L_e^2 L_u$  for types  $\mathcal{T}_5$  and  $\mathcal{T}_6$ .

#### 4.2. Analyses of simulated catalogs

We randomly distribute 50 cosmic objects within the fundamental cell and we calculate the ghost images in the universal covering space, to simulate the appearance of the sky up to a redshift cut-off  $z = 4$ . For galaxy clusters, we neglect the peculiar motions which could slightly deviate the positions of ghosts from a rigorous distribution.

In a first series of simulations we have chosen equal edges  $L_e = L_a = L_u$ , adjusted so that the fundamental cell has a volume  $(1500 h^{-1} \text{Mpc})^3$ . According to Table 1, the number of ghosts is about 45 times the number of originals. Ghosts appear at  $z > 0.31$  and originals disappear at  $z > 0.63$ . Figure 1 shows the 2-dimensional appearance of the sky. Fake large-scale structures are generated but, as expected, no information about multi-connectedness appears.

We have also plotted in Fig. 2 the histogram of redshifts, calculated for the hypertorus model. No periodic pattern nor any sign of multi-connectedness appears. This confirms former simulations by Ellis and Schreiber (1986) and the statements by LaLu95 according to which such histograms cannot provide a valuable test for cosmic topology.

Next, for each simulated catalog of objects we have drawn the pair separation histogram. They are displayed in Fig. 3, from which the information about multi-connectedness and the topological type spectacularly springs out.

Spikes, which gather all gg-pairs linked by holonomies, appear at squared separations  $\Lambda_i$  obeying to Eq. (1). A straightforward calculation of the separations between  $(x', y', z')$  and  $(x, y, z)$  according to Eqs. (2–4) and Table 2 shows that Eq. (1) may be rewritten under the very simple form

$$n_e^2 + n_a^2 + n_u^2 = \frac{\Lambda_i^2}{V^{2/3}} \quad (5)$$

for the triplets on integers  $(n_e, n_a, n_u)$  compatible with the topology. The values of  $n$  span a range limited by the finite size of the catalog (0 to 5 in our calculation). For a given topology the positions of spikes are displayed in Table 3.

For a better understanding of Table 3, let us comment in more details the spectrum of spikes obtained for types  $\mathcal{T}_1$  (cubic hypertorus) and  $\mathcal{T}_4$ . For  $\mathcal{T}_1$ , the holonomies are generated by the three translations along the edges of the parallelepipedic cell, with magnitude  $L = V^{1/3}$ . In such a simple lattice structure, all the triplets of integers  $(n_e, n_a, n_u) \in \{0, \dots, 5\}$  realize an holonomy. Spikes thus appear at all locations  $\Lambda_i$  such that  $\Lambda_i^2/V^{2/3}$  is the sum of three squared integers. Most integers except 7, 15, 16... are solutions. For  $\mathcal{T}_4$ , the holonomies are generated by two translations and a glide reflection. For such a lattice structure, only a few triplets of integers  $(n_e, n_a, n_u)$  realize an holonomy, so that Eq. (5) has much less solutions.

Let us also examine the amplitude of the spikes. For type  $\mathcal{T}_1$  for instance, the spike at position  $\Lambda_i^2/V^{2/3} = 1$  is generated by the contributions of the triplets (1, 0, 0), (0, 1, 0) and (0, 0, 1), whereas the spike at position  $\Lambda_i^2/V^{2/3} = 5$

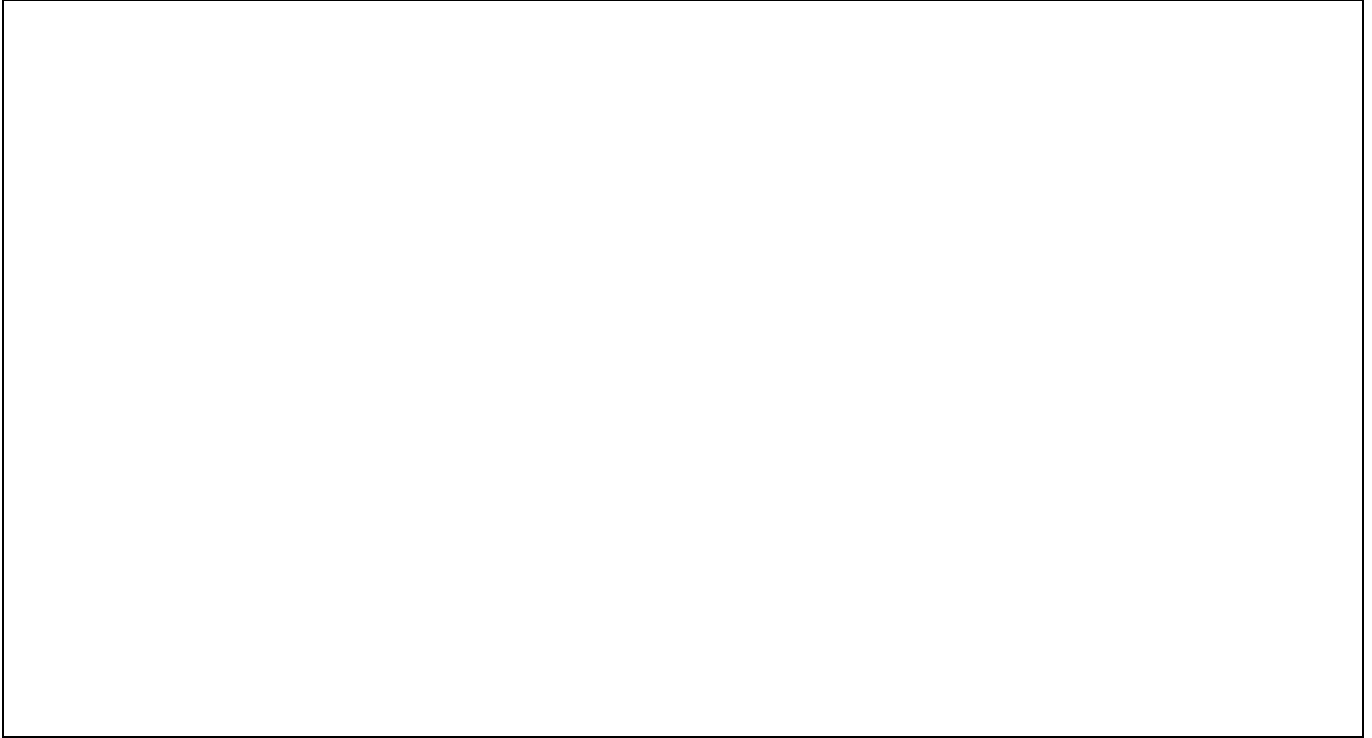


**Fig. 1.** Appearance of the sky (equal area projection) in an Einstein–de Sitter universe with topology  $\mathcal{T}_1$ . The fundamental polyhedron is a cubic hypertorus whose size is  $1500 h^{-1}$  Mpc.

is generated by the triplets  $(2, 1, 0)$ ,  $(2, 0, 1)$ ,  $(1, 2, 0)$ ,  $(1, 0, 2)$ ,  $(0, 1, 2)$  and  $(0, 2, 1)$ . Thus, spike 5 is more intense than spike 1. All the characteristics of Table 3 can be described in a similar way. We conclude that the very existence of spikes reveals the multi-connected nature of topology, whereas their positions and amplitudes discriminate the topological types.

We also performed the simulation in a toroidal model like  $\mathcal{T}_1$ , but with unequal identification lengths. Figure 4 shows the result for  $L_a$ ,  $L_e = \sqrt{2} L_a$ , and  $L_u = \sqrt{3} L_a$ , so that  $V = (1500 h^{-1} \text{Mpc})^3$ . The lengths being not commensurable, the spikes are more numerous, corresponding to all positions fundamental lengths and there multiples, but less intense since no gg-pair corresponding to different  $\Lambda_k$  accumulate in a same spike.

Our simulated catalogs are however highly idealized so that the spikes due to gg-pairs stand out dramatically above the background distribution of other pairs. In a more realistic distribution, it would be more difficult to recognize the spikes, since various effects would contribute to spoil the sharpness of the spikes and decrease the signal to noise ratio. For instance, the real catalogs do not include the region masked by the galactic plane, and cover only a small area of the sky. In order to examine the consequences of this, we also created a catalog, in a simulated small folded universe, which is of limited solid angle. We observe that the signal fades out when the aperture angle of the catalog goes down to about  $20^\circ$  (see Fig. 5).

Also, clustering in a simply-connected universe can generate noise spikes that mimic spikes due to multi-connectedness. For instance, the spikes in the pair separation histograms shown in the Broadhurst et al. sample (1990) and in the Parks and Gott (1991) simulations are due to noise. More precisely they are caused by the large number of pairs relating the many galaxies in a first cluster to those in a second cluster, all at the cluster separation. Generally, such spikes currently also occur in N-body simulations that show clustering.

## 5. Results and discussion

### 5.1. Analysis of a cluster catalog

We have applied our test to a 3-dimensional catalog of galaxy clusters compiled by Bury (private communication). This catalog includes all Abell and ACO clusters with published redshifts. It contains 901 clusters, up to a maximal redshift  $z_{max} \approx 0.35$ , corresponding to  $840 h^{-1}$  Mpc in an Einstein–de Sitter universe (although only 12 objects have

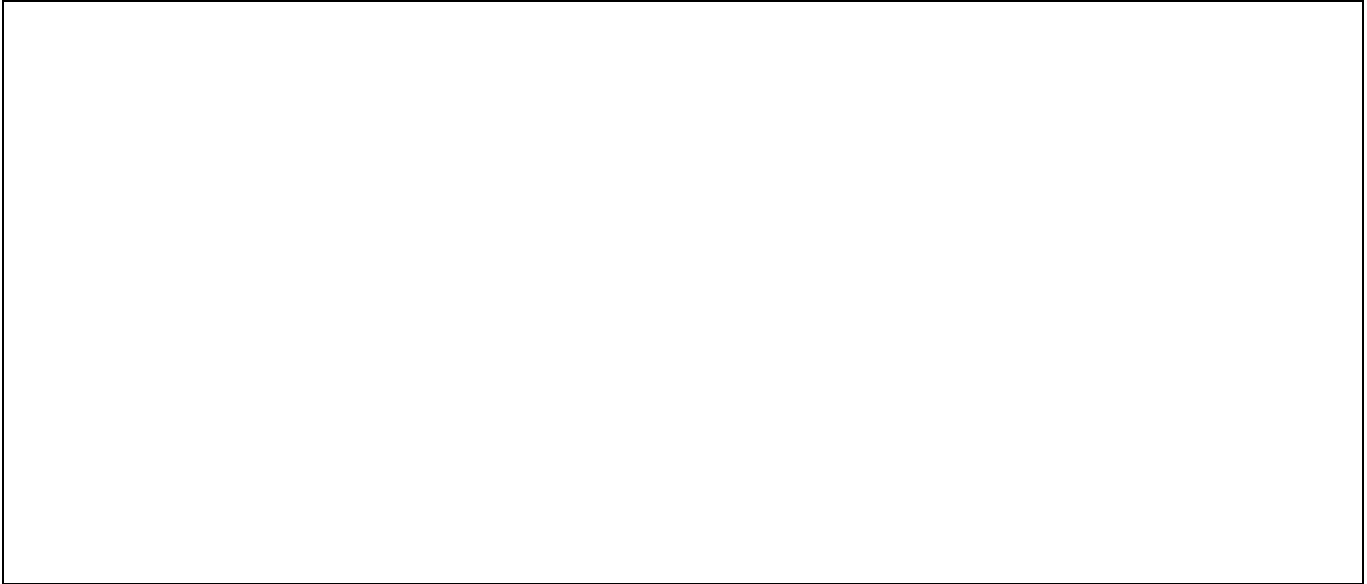


**Fig. 2.** The redshift histogram generated by 50 randomly distributed objects in the fundamental cell of a  $\mathcal{T}_1$  universe.

**Table 3.** The spike's spectrum of small folded Euclidean universes. The rank of the three stronger spikes are denoted by the exponent.

$\mathcal{T}_1$	$\mathcal{T}_2$	$\mathcal{T}_3$	$\mathcal{T}_4$	$\mathcal{T}_5$	$\mathcal{T}_6$
1	1	$1^2$	–	–	–
$2^3$	2	$2^3$	–	–	–
3	–	–	$3^1$	$3^1$	$3^1$
4	$4^3$	–	$4^2$	–	–
$5^1$	$5^1$	$5^1$	–	–	–
$6^2$	6	–	–	–	–
–	–	–	–	7	$7^3$
8	8	8	$8^3$	–	–
9	$9^2$	9	–	$9^2$	$9^2$
10	10	10	–	–	–
11	–	–	11	–	–
12	12	–	12	$12^3$	12
13	13	13	–	13	13
14	14	–	–	–	–
–	–	–	–	–	–
–	16	–	–	16	16
17	17	17	–	–	–
–	–	–	–	18	–
–	–	–	–	19	19
–	–	–	–	–	–

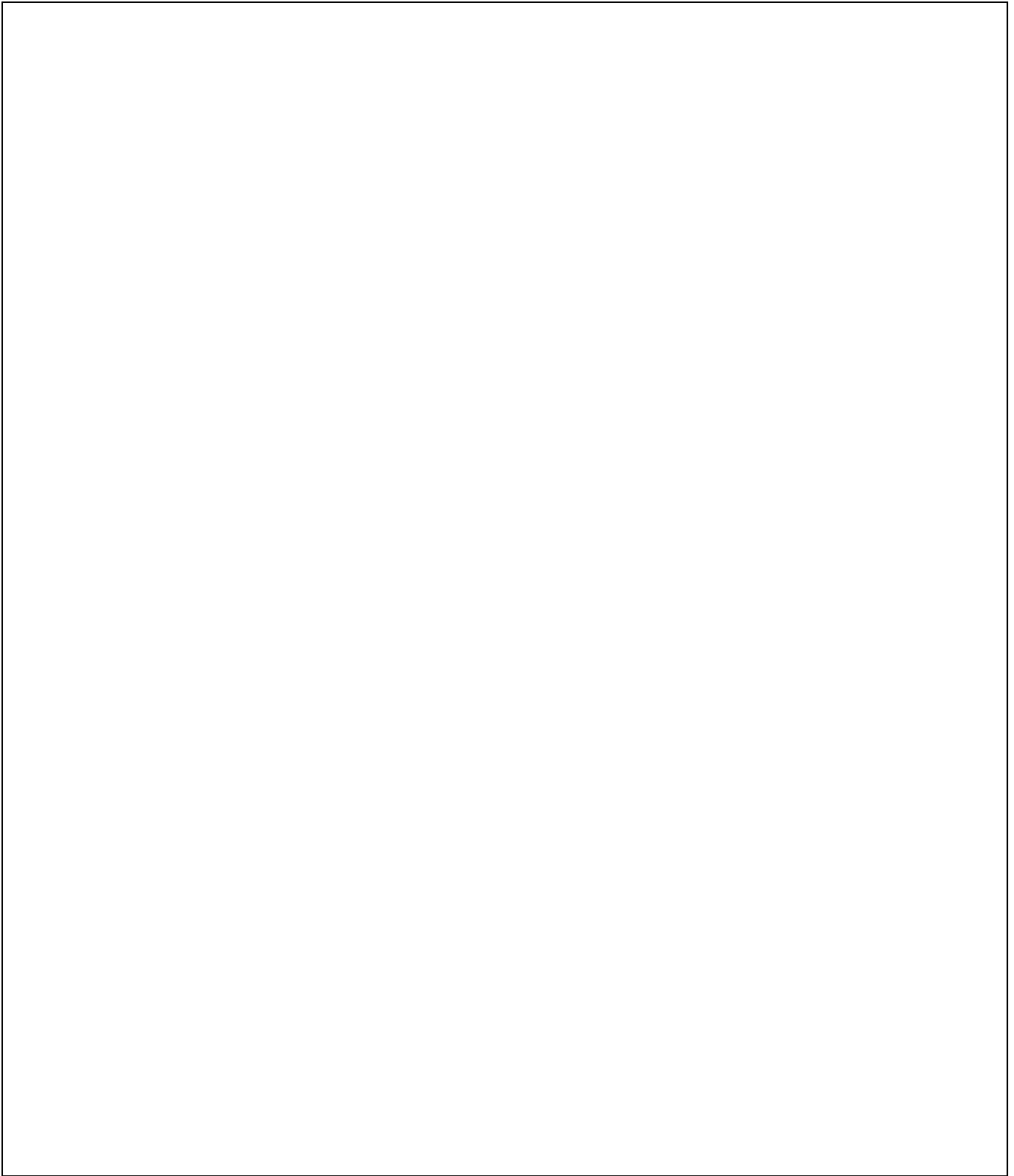


**Fig. 3.** Histogram of squared separation distances between all pairs of images for the 6 topological types, with equal lengths. The spikes reveal repetition scales related to the size of the fundamental polyhedron.





**Fig. 4.** Histogram of squared separation distances for a  $\mathcal{T}_1$  universe with unequal lengths.

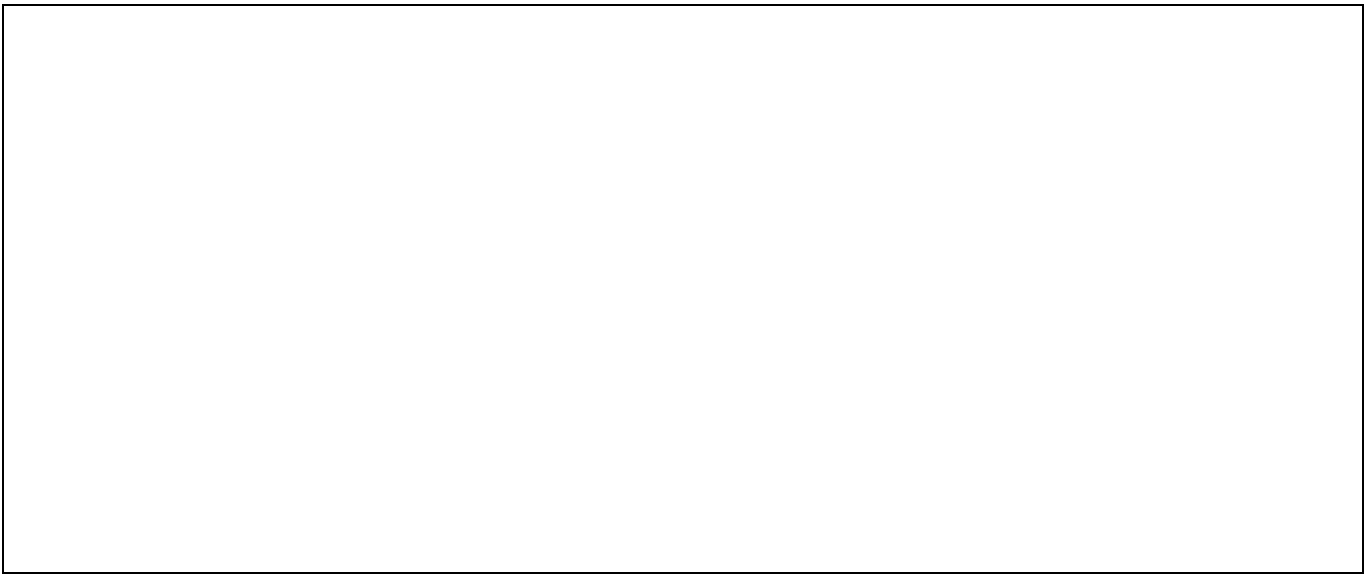
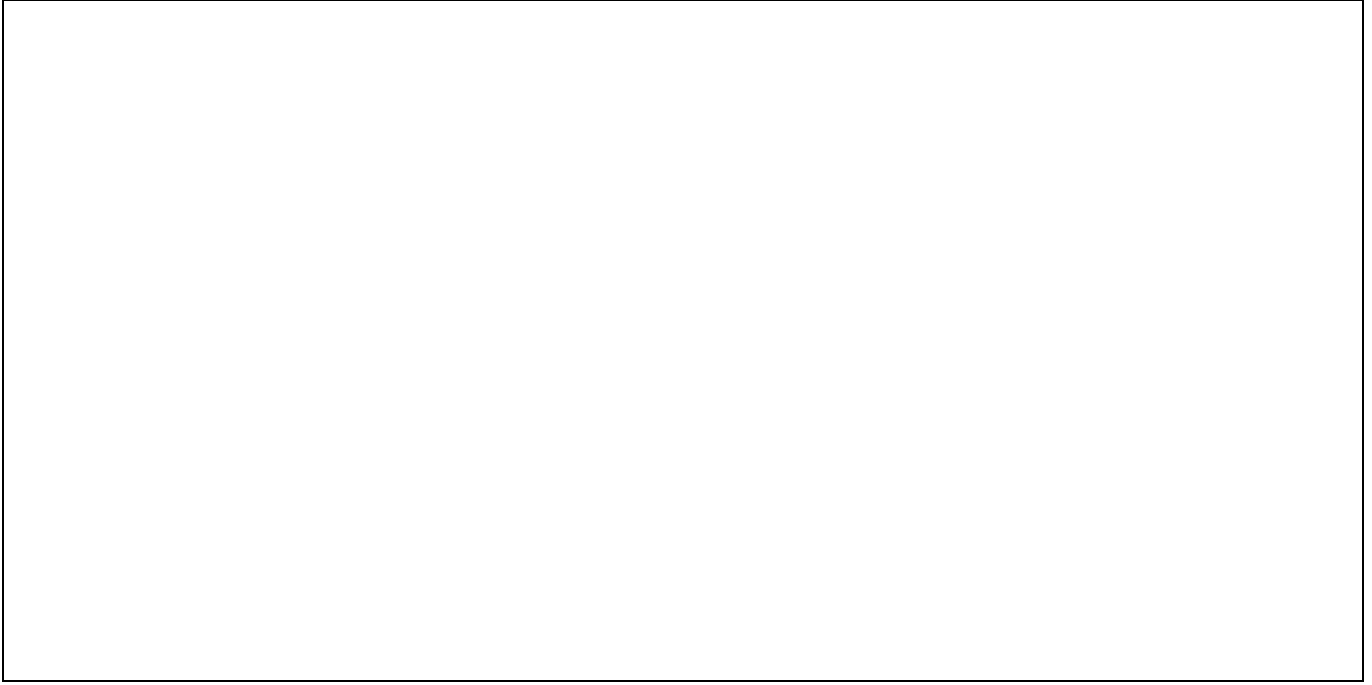


**Fig. 5.** Histogram of squared separation distances inside a conical catalog of aperture angle  $20^\circ$ , for a  $\mathcal{T}_1$  universe with equal lengths.

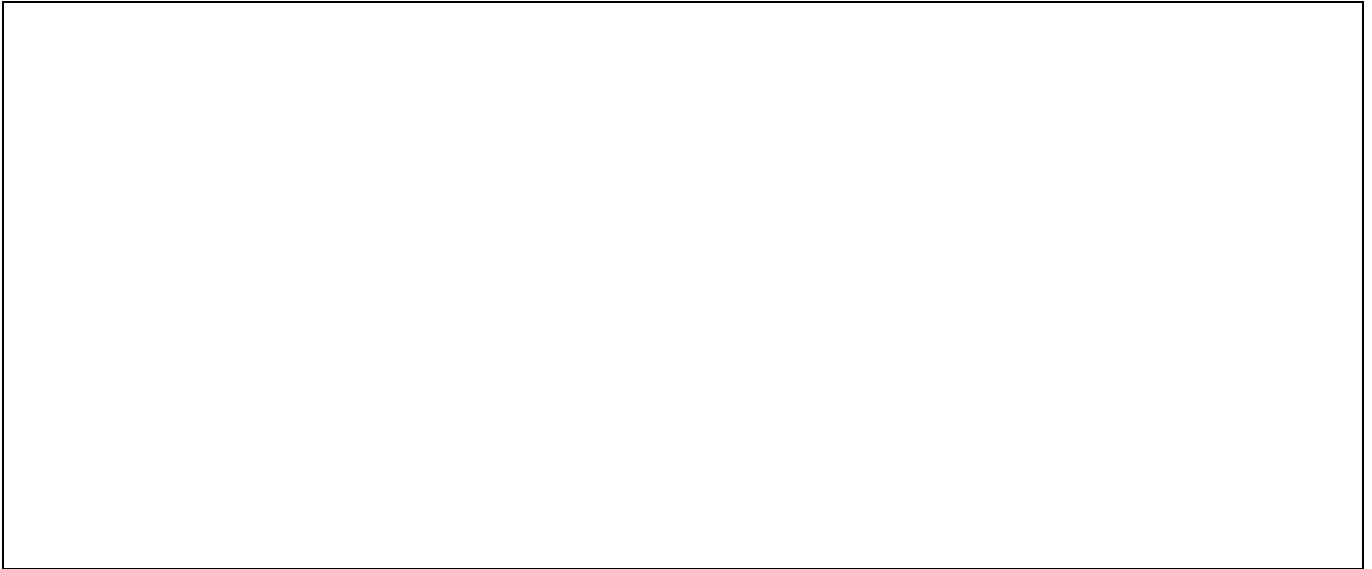
$z > 0.26$ ). Due to obscuration by the galactic plane, the shape is a double cone of aperture  $\approx 120^\circ$ , sufficient to allow the desired effects to be observable. Figure 6 shows its projection onto the sky.

Figure 7 presents the histogram of separations where two suspicious spikes are detected corresponding to separation of  $270 h^{-1}$  Mpc and  $382 h^{-1}$  Mpc. The ratio of these quantities is very near  $\sqrt{2}$ . If those spikes are really due to topology, this means that we are seeing multiple images of some given objects. In order to check this hypothesis, we have first simulated the Bury catalog: we distributed randomly 30 objects in a fundamental cell with  $L_e = L_a = L_u = 270 h^{-1}$  Mpc, put a redshift cut-off at  $z = 0.26$ , and limited our set of ghosts by a double cone of aperture  $120^\circ$ . The number of real objects is chosen to obtain 901 ghosts in the final catalog. Then, we plot the histogram of separation on Fig. 8.

The comparison with Figs. 7 leaves no room to doubt. Multi-connectedness at a scale  $\approx 270 h^{-1}$  Mpc would give a much stronger signal than observed. To check further, we also selected all pairs contributing to the observed spikes. Were they due to multi-connectedness, then the associated separation vectors would clump in preferred directions,



**Fig. 6.** Two dimensional equal area projection onto the sky of the Bury cluster catalog.



**Fig. 7.** Histogram of squared separation distances for the Bury cluster catalog.

corresponding to the principal directions. Clearly, this is not the case as indicated by Fig. 9. Thus the observed spikes are only due to noise and no effect of multi-connectedness appears. Given the depth of the catalog, we conclude to the limit  $\alpha > 650 h^{-1}$  Mpc, comparable to those already obtained from large scale objects distribution. However applications of our test will be decisive when deeper 3D catalogs are available. Current observational programs devoted to extended redshift surveys will offer this possibility within the next decades.

### 5.2. Conclusion

We have presented a new method to check and characterize a possible multi-connectedness of space on sub-horizon scales. Our test is free of specific assumptions about the geometry and the topological type. It is based onto the

simple fact that a displacement carrying a ghost image to another of the same object is an isometry in the universal covering space. Thus, in a multi-connected space, we expect that the histogram of all pair separations between objects of a large 3-dimensional catalog exhibits strong spikes, corresponding to combinations of the identification scales. Numerical simulations performed on Euclidean “small folded” universe have shown that the relative positions and amplitudes of the spikes characterize in an unique way the topological type: different topologies generate different recognizable spikes structures. Applying this test to present 3-dimensional catalog of galaxy clusters does not provide new limits on the lower size of the universe.

Taking into account various effects such as luminosity evolution, peculiar velocities and clustering of real objects within the fundamental cell would not change the value of our test. In the future, it will be interesting to apply the test to more extended catalogs, and to collections of objects of different types. Note also that the test can be made still more efficient by considering pairs of specific configurations rather than isolated objects, like strings of images with a given shape.

In the case of a significant distortion, the pair separation histogram would also provide a powerful and purely geometrical method to determine the sign of the curvature of space. This results from the fact that the crystallographic structures of the holonomy groups differ for the cases  $k = 1, 0, -1$ . Thus, beside its own specific interest, multi-connectedness could bring an answer to a long-standing problem of observational cosmology.

*Acknowledgements.* We thank the anonymous referee for useful comments on the first manuscript and Bury for providing us his clusters catalog.

## References

- Broadhurst, T.J., Ellis, R.S., Koo, D.C. & Szalay, A.S., 1990, *Nature*, 343, 726  
Ellis, G.F.R., 1971, *Gen. Rel. Grav.* 2, 7  
Ellis, G.F.R. & Schreiber, 1986, *Phys. Lett. A* 115, 97–107  
Fagundes, H.V., 1995, preprint IFT-P.050/95  
Fang, L.Z., 1990, *A&A* 239, 24  
Fang, L.Z., & Liu, Y. L., 1988, *Mod. Phys. Lett. A*, 13, 1221  
Gott, J. R., 1980, *Mon. Not. R. Astr. Soc.* 193, 153  
Jing, Y.P. & Fang, L.Z., 1994, *Phys. Rev. Lett.* 73, 1882  
Lachièze-Rey, M. & Luminet, J.P., 1995, *Phys. Rep.* 254, 135–214  
de Oliveira-Costa A. & Smoot G. F., 1995, *Ap. J.* 448, 477  
Park, C. & Gott, J.R., 1991, *Mon. Not. R. Astr. Soc.* 249, 288  
Sokoloff, D.D. & Shvartsman, V.F., 1974, *Sov. Phys. JETP*, 39, 196  
Starobinsky, A.A., 1993, *JETP Lett.* 57, 622  
Stevens, D., Scott, D. & Silk, J., 1993, *Phys. Rev. Lett.* 71, 20